

# First-Principles Study of the Electronic Structure and Cluster Formation in Expanded Liquid Boron

Wataru Hayami\*

Advanced Nanomaterials Laboratory, National Institute for Materials Science, 1-1 Namiki, Tsukuba, Ibaraki 305-0044, Japan

Received: January 23, 2009; Revised Manuscript Received: March 27, 2009

The electronic structure of liquid boron and cluster formation in expanded liquid boron have been investigated with first-principles molecular dynamics simulations. The calculated electronic density of states (DOS) exhibits a metallic feature, while liquid boron is known experimentally to be semiconductive. Since the DOS is not very sensitive to density, the electronic states near the Fermi level will consist mainly of dangling bonds, which explains the difference between the calculated and experimental results. Many types of clusters are formed in expanded liquid boron. This formation occurs in a very different way from that at low temperatures because expanded liquid boron has a high temperature and pressure that are close to the liquid–gas critical point. As the density is reduced, the coordination number in boron clusters decreases to about 2, indicating that the cluster geometry tends to be one- rather than two-dimensional, which is the most stable form at low temperatures. In fact, the analysis of small clusters proved that one-dimensional forms are dominant over two- and three-dimensional forms. This is because one-dimensional geometries have a more flexible structure and a high entropy value that consequently reduces the free energy at high temperatures.

## Introduction

Solid boron is a semiconductive material under normal conditions and has various polymorphs. Two rhombohedral ( $\alpha$ ,  $\beta$ ) and two tetragonal ( $\alpha$ ,  $\beta$ ) structures are well-known in which icosahedral B<sub>12</sub> units construct the framework of the structure.<sup>1</sup> Although boron has been studied for many years, it has attracted relatively little attention compared with other semiconductors such as silicon, probably because the industrial applications of elemental boron are limited. However, the situation has been changing since the recent discovery of superconductivity in MgB<sub>2</sub><sup>2</sup> and in elemental boron under high pressure.<sup>3</sup> In addition, progress in nanotechnology has made it possible to synthesize a boron nanotube,<sup>4</sup> which is expected to exhibit metallic conductivity.<sup>5</sup>

Although there have been many studies on solid boron, there have been few on liquid boron. The melting point of boron is as high as 2360 K,<sup>6</sup> which makes experiments on liquid boron very difficult to perform. Computer simulations can avoid such experimental difficulties, and Vast et al. conducted a pioneering study on liquid boron using first-principles molecular dynamics (MD) simulations.<sup>7</sup> They obtained two important results. First, liquid boron does not retain its icosahedral B<sub>12</sub> units on melting. This supports the previous finding from vibration analysis that the intericosahedral bonds are stronger than the intraicosahedral bonds.<sup>8,9</sup> Second, the electronic density of states (DOS) of liquid boron exhibits a metallic feature and the estimated dc conductivity is  $2.5 \times 10^4$  ( $\Omega$  cm)<sup>-1</sup>.

An experimental breakthrough was made by Krishnan et al.<sup>10</sup> using the gas levitation technique. This approach maintains a droplet of liquid boron in the air using an Ar gas flow thus avoiding the need to employ any sample containers. They measured the radial distribution function and found that the coordination number does not change greatly on melting. The density of liquid boron was measured by Millot et al.<sup>11</sup> using

the same method and by Paradis et al.<sup>12</sup> using the electrostatic levitation method. Both groups reported that the boron density increases slightly on melting. Glorieux et al. reported on the conductivity of liquid boron.<sup>13</sup> They positioned a coil around a gas levitated boron droplet and measured the ac conductivity. Contrary to the theoretical prediction by Vast et al.,<sup>7</sup> the conductivity fell in the semiconductor range, namely,  $960 \pm 80$  ( $\Omega$  cm)<sup>-1</sup>. Millot et al.<sup>11</sup> suggested that the disagreement with the theoretical result was due to the fact that the boron density adopted in the MD simulations was less than that in their experiment. To examine the cause for the difference between the experimental and theoretical results, the first aim of this study was to recalculate the DOS of liquid boron over a wide density range.

The second and main aim was to understand the cluster formation in thermodynamic fluid boron. Atomic clusters are generally formed in boron in its liquid and gas phases. Boustani et al. used ab initio calculations to reveal that for boron clusters planar structures are more stable than three-dimensional structures and they have metallic properties.<sup>14</sup> Later, Zhai et al. discovered such planar structures experimentally in boron clusters vaporized with a laser beam and then cooled in helium gas.<sup>15</sup> These theoretical and experimental studies dealt with clusters at zero or low temperatures, and it is not known what species of clusters are formed in real liquid and gas boron. In a liquid state at normal density, most boron atoms are likely to be connected and there will be few isolated clusters. On the other hand, in a gas state at normal pressure, the density is too low for large clusters to form. Therefore, it is interesting to investigate a medium density state, i.e., an expanded liquid or a dense gas near the liquid–gas critical point (CP), where many types of clusters are expected to form owing to the large density fluctuation.

For covalent materials such as boron, the temperature and pressure of the CP are extremely high and have yet to be determined experimentally. The critical temperature will be

\* E-mail: hayami.wataru@nims.go.jp.

several times higher than the boiling point. It is also difficult to predict precisely the CP parameters from first-principles MD simulations and no such data are available for boron. However, we can define both the temperature and the density in MD simulations and determine whether the system is in a uniform liquid, gas, or a supercritical state, as explained later.

Thus, we conducted well-defined first-principles MD simulations of expanded liquid boron to investigate the cluster formation at given temperatures and densities near the CP. The density was reduced to a fourth of its normal value. The behavior of clusters at high temperatures was found to be very different from that at low temperatures.

### Computational Details

The first-principles MD simulations were conducted using the CPMD code, version 3.9.1.<sup>16,17</sup> This code is based on the density functional theory and the Car–Parrinello method using plane waves and pseudopotentials.<sup>18–20</sup> The norm-conserving Troullier–Martins-type pseudopotential was used.<sup>21</sup> The generalized gradient approximation was included by using the functional derived by Becke<sup>22</sup> and by Lee, Yang, and Parr.<sup>23</sup> An energy cutoff of 40 Ry was sufficient to provide convergence of the total energies and geometries.<sup>24</sup> It was confirmed that this condition reproduced the relative stability of small clusters dealt with in ref 14.

The Car–Parrinello MD simulations were performed only at the  $\Gamma$  point with spin-restricted wave functions. There may be some spin effects for  $B_2$  dimers but not for larger clusters because highest occupied molecular orbitals (HOMOs) are not generally degenerated. One hundred twenty eight atoms were contained in a cubic unit cell with periodic condition. Then the density was determined by the size of the unit cell assuming the atomic weight of boron to be 10.811. The temperature of the system was controlled by scaling the total kinetic energy of the atoms at every time step. The time step was 5.0 au (0.121 fs), and each simulation for cluster analysis consisted of 16000 steps. All the tasks were executed on a parallel computer (Hitachi SR11000) using a message-passing interface.

Before performing the MD simulations, we needed to know the pressure of the system because we had to clarify where the system was located on the liquid–gas phase diagram of boron. The pressure was estimated at a given temperature and density by employing first-principles Parrinello–Rahman molecular dynamics<sup>25,26</sup> using the same code. This technique is usually used to conduct isobaric MD simulations, where the lattice parameters of the unit cell are allowed to vary to equilibrate the internal stress with respect to the external applied pressure. Here, we utilized the Parrinello–Rahman Lagrangian solely to extract the internal stress tensor under constant unit cell parameters. We achieved this by setting the fictitious mass of the unit cell at a very high value. The total internal stress tensor is the sum of the contribution from the thermal motion of atoms and the electronic stress tensor,<sup>27</sup> from which the internal pressure is calculated. The internal stress tensor fluctuates statistically at every time step. Therefore, we used about 4000–6000 steps to average the internal stress tensor, i.e., the internal pressure. The absolute value of the internal pressure may involve errors caused by the approximations, but as explained later, the pressure–volume curve tells us whether or not the system is in a uniform state, i.e., not in a liquid–gas coexistence state.

### Results and Discussion

First, we calculated the DOS of liquid boron at 2600 K with densities of 1.6–2.6 g/cm<sup>3</sup>. The temperature is above the melting

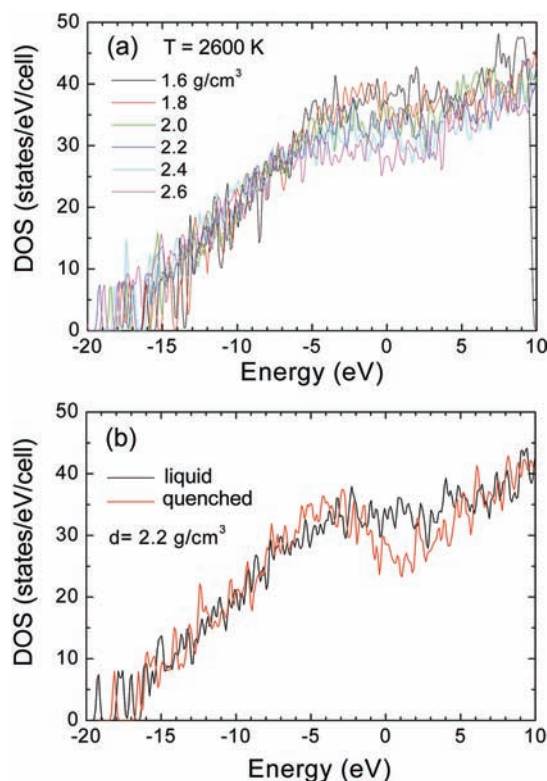


**Figure 1.** (a) DOS of liquid boron at 2600 K. (b) DOS of liquid boron and quenched amorphous boron.

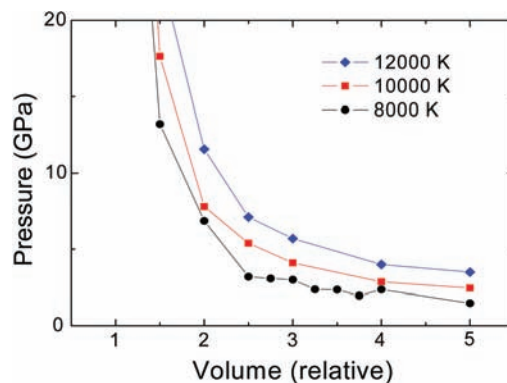


**Figure 2.** Volume–pressure curves of liquid boron. The unit of volume is 1044.4 Å<sup>3</sup>, corresponding to the density of 2.2 g/cm<sup>3</sup>.

point (2360 K), and the density covers the experimental values of 2.17 and 2.33 g/cm<sup>3</sup>.<sup>11,12</sup> The results are shown in Figure 1a. The Fermi level is set at zero. The atomic coordinates were those after 4000 steps (96.8 fs) from the start of MD, and they were in an equilibrium state. The DOSs appear to be metallic for all the densities. The results are somewhat similar to those reported by Vast et al., but the decrease in DOS around the Fermi level is not as large as they observed. However, according to the experiments undertaken by Glorieux et al.,<sup>13</sup> the electric conductivity of liquid boron at this temperature is not metallic but semiconductive. Millot et al.<sup>11</sup> attributed the difference between their experimental result and the calculation reported by Vast et al.<sup>7</sup> to the fact that Vast et al. adopted a density of 2.0 g/cm<sup>3</sup> that was lower than their experimental value of 2.33 g/cm<sup>3</sup>.

However, this is incorrect because our calculations show that the DOSs of liquid boron are always metallic whatever the density in the 1.6–2.6 g/cm<sup>3</sup> range. Therefore, we conclude that the calculated electronic states around the Fermi level are

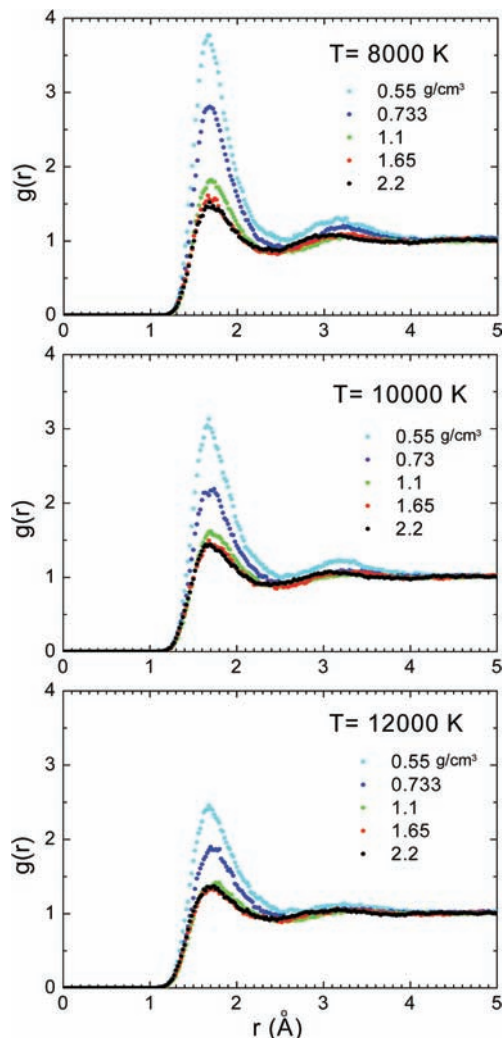


**Figure 3.** Radial distribution functions  $g(r)$  of liquid boron.

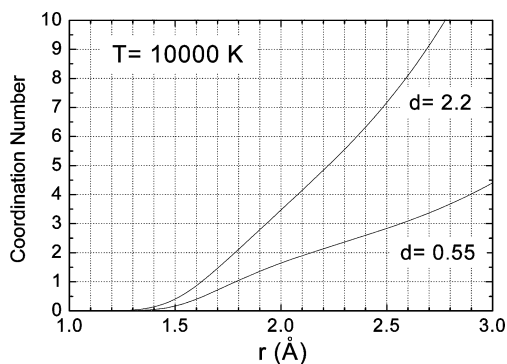


**Figure 4.** Coordination number of liquid boron as a function of cutoff distance.

localized, probably because they consist mainly of dangling bonds. To confirm this, we optimized the liquid boron geometry at zero temperature, i.e., rapidly quenched the liquid, and recalculated the DOS (Figure 1b). The atomic structure was amorphous. The DOS around the Fermi level decreased by about 30%, which means that some of the dangling bonds had disappeared as a result of the formation of new bonds. The DOS does not decrease to zero since the structure is amorphous and a large number of dangling bonds still remain.

For MD simulations of expanded liquid boron, it is necessary to set the system near the liquid–gas CP. The problem is that the CP of boron has yet to be determined experimentally. With

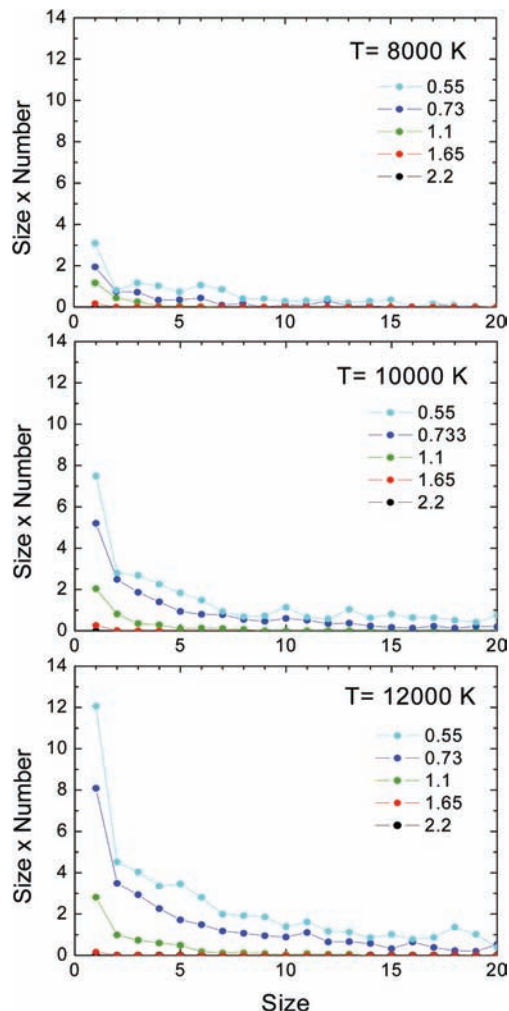


**Figure 5.** Distributions of boron clusters. The size means the number of atoms in a cluster.

the exception of molecular materials, the CP is known only for certain elements including Na, K, Rb, Cs, Hg, and Se.<sup>28</sup> All of these elements have low melting and boiling points. According to classical MD using a Lennard-Jones potential,<sup>29</sup> the CP temperature is proportional to the depth of the potential. Since the cohesive energy of boron is several times higher than that of alkali metals, the CP temperature must be very high and would be difficult to determine experimentally. It is also difficult to calculate CP parameters from first principles.

Although the liquid–gas phase diagram is not available, it is possible to judge whether or not the system is in a uniform state. When temperature  $T$ , volume  $V$ , and atom number  $N$  are given in an MD simulation, the pressure  $P$  is obtained from the total internal stress tensor, as mentioned in the previous section. The statistical error of  $P$  is sufficiently diminished as the simulation goes through several thousand time steps. Figure 2 shows the pressure of liquid boron as a function of  $V$ . The MD simulations included 128 atoms in a cubic unit cell under a periodic condition. The unit of volume is  $1044.4 \text{ \AA}^3$ , which gives a normal density of  $2.2 \text{ g/cm}^3$ . The pressure, given in gigapascals, is meaningful only in terms of relative variance.

When  $T = 8000 \text{ K}$ ,  $P$  rapidly decreases from  $V = 1.0$  to  $2.5$  and then discontinuously changes its gradient and becomes rather flat until  $V = 4.0$ . This suggests that the phase transition occurs around  $V = 2.5$  and the system becomes a liquid–gas coexistence phase. When  $T = 10000$  and  $12000 \text{ K}$ , there is no discontinuous change in the gradient from  $V = 1.0$  to  $5.0$ ,



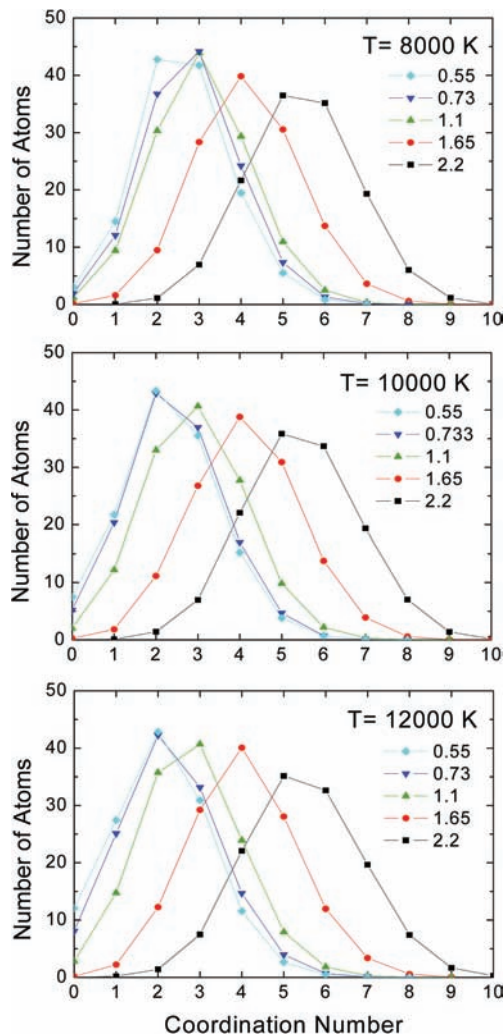
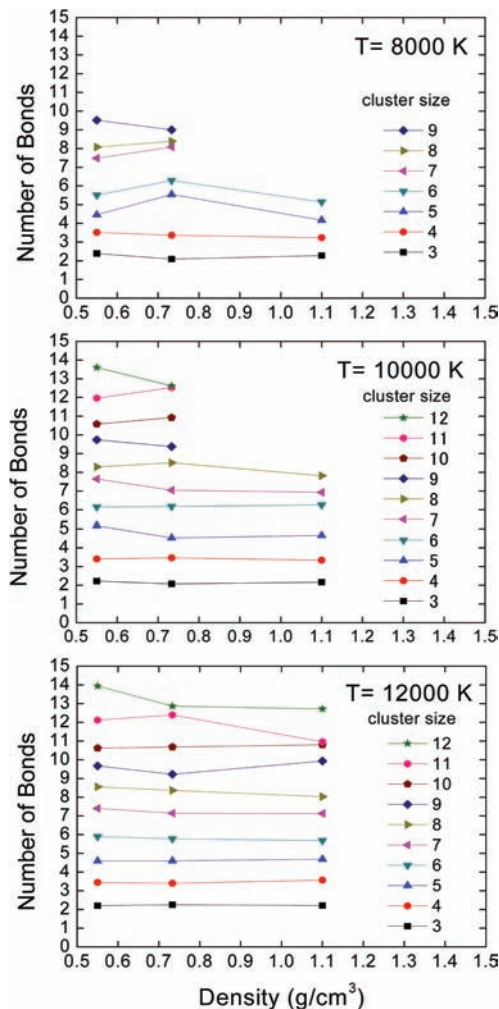


**Figure 6.** Distribution of the coordination numbers of liquid boron.

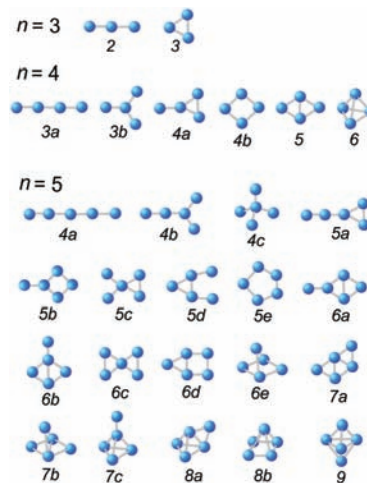
suggesting that the system has no phase transitions and the density is uniform. The temperature is probably above the CP in these cases. On the basis of these considerations, we investigated expanded liquid boron at volumes of 1.0–4.0, corresponding to densities of 2.2–0.55 g/cm<sup>3</sup>, at temperatures of 8000, 10000, and 12000 K.

Figure 3 shows radial distribution functions of liquid boron. It should be noted that the states with  $d = 0.733$  and  $0.55$  g/cm<sup>3</sup> at 8000 K are a liquid–gas coexistence phase as mentioned above. For all temperatures, the first peaks occur at about 1.7 Å and do not depend greatly on the density. The second peaks are broad and occur around 3.2 Å. The first peaks increase as the density decreases, meaning that the number of neighboring atoms increases relatively to the average density as the atoms cluster. This does not necessarily mean an increase in the coordination number because the density itself is reduced. An analysis of the coordination number will be provided later. At the same density, the height of the first peak decreases as the temperature increases. This is because the thermal motion of atoms becomes intense as the temperature increases. This effect is clearer when the density is low.

For a cluster analysis, it is necessary to determine the cutoff distance for interatomic bonds. The choice of cutoff distance is arbitrary to some extent. Figure 4 shows the number of neighboring atoms (coordination number) as a function of the cutoff distance at 10000 K and  $d = 2.2$  g/cm<sup>3</sup>. The first minimum in the distribution function (Figure 3) is at about 2.4



**Figure 7.** Average numbers of bonds in a boron cluster as a function of density.



**Figure 8.** Possible forms of small ( $n = 3$ – $5$ ) boron clusters.

Å, but the coordination number at this distance is 6.3, which is higher than that in  $\alpha$ -rhombohedral ( $\alpha$ -rh) boron. For  $\alpha$ -rh boron, the bond length to the nearest neighbor is around 1.7–1.8 Å, and then the coordination number is 5.5. The second nearest neighbors are at about 2.0 Å, but in terms of electron density, the bonds to the second nearest neighbors are very weak.<sup>30</sup> In the experiment undertaken by Krishnan et al., the liquid boron coordination number is 5.8.<sup>10</sup> Therefore, we adopt a cutoff distance of 2.3 Å, which gives a coordination number of 5.55.

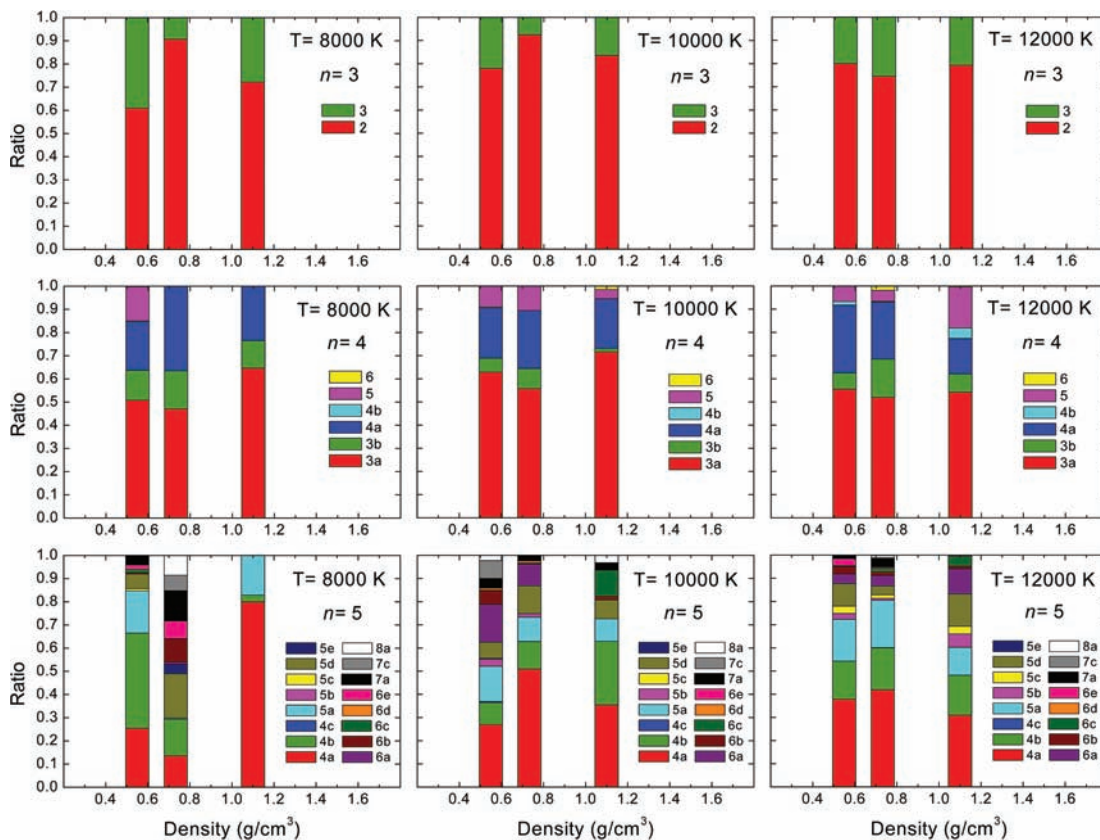


**Figure 9.** Distribution of forms of boron clusters ( $n = 3-5$ ).

The positions of the first minimum shift slightly toward larger distances as seen in Figure 3. At 10000 K, for example, it shifts from 2.4 Å ( $d = 2.2$ ) to 2.5 Å ( $d = 0.55$ ). The exact value that should be adopted for the cutoff distance of low-density liquid boron is not known because no experimental data are available. Therefore, the same cutoff distance of 2.3 Å was adopted in all cases. This approximation is acceptable since when  $d = 0.55$  g/cm<sup>3</sup>, for example, a difference of 0.1 Å in distance yields a difference of 0.25 (about 10%) in the coordination number at 2.3 Å (Figure 4).

Figure 5 shows the cluster size distribution. Here, the size means the number of atoms in a cluster. The ordinate shows the average number of clusters multiplied by the size that appear in the unit cell (128 atoms). For all the temperatures, densities above 1.65 g/cm<sup>3</sup> provide no clusters, which means the atoms in a system are all connected within the cutoff distance. Clusters begin to appear at a density of 1.1 g/cm<sup>3</sup>, or half the normal density. The number of clusters depends greatly on the temperature. At 8000 K, the number of clusters is so small that the statistical error is large. The number of clusters decreases monotonically as the size increases, and no magic numbers are observed. Large clusters ( $>5$ ) occur when the density is lower than about 0.733 g/cm<sup>3</sup>, or a third of the normal density.

The coordination number distributions are shown in Figure 6. For all temperatures and at the normal density of 2.2 g/cm<sup>3</sup>, the peaks are around 5–6 and the shapes are almost the same. Very few coordination numbers are larger than 9. At densities above 1.1 g/cm<sup>3</sup>, coordination numbers of 0 and 1 rarely appear, indicating that the most of the atoms are connected and isolated clusters are not formed at these densities. These low coordination numbers increase as the temperature increases because the number of clusters increases with temperature as seen in Figure 5. The coordination numbers decrease as the density decreases. It is interesting that curves with  $d = 0.733$  and 0.55 g/cm<sup>3</sup> are

almost the same at  $T = 10000$  and 12000 K, with a peak around 2. This suggests that the connection of atoms is becoming one-dimensional. At zero temperature, as mentioned above, boron clusters are the most stable when they have planar structures.<sup>14</sup> Then the coordination number should typically be 6 for inner atoms and 3 for edge atoms. Therefore, the cluster geometry should be very different in expanded liquid boron at high temperatures.

For a more quantitative analysis, the numbers of bonds in each cluster were counted as shown in Figure 7. For a density of 1.1 g/cm<sup>3</sup> at 8000 and 10000 K, the numbers of large clusters are very small and involve a large statistical error, so they are partly omitted from the graphs. It is surprising that the numbers of bonds for each cluster size do not depend greatly on density or temperature. This does not in fact contradict the variation of the coordination number in Figure 6. The coordination numbers in Figure 6 include the contribution from the connected mass of atoms. At densities higher than 1.65 g/cm<sup>3</sup>, most of the atoms are connected and have a large coordination number.

If a cluster of size  $n$  is completely linear, or consists of only linear branches, it has  $n - 1$  bonds. The numbers of bonds in Figure 7 are about  $n - 1$  to  $n$  when  $n$  is 6 or less. Even when  $n$  is higher than 6, the numbers of bonds remain in the range between  $n$  and  $n + 1$ . Therefore, most clusters are considered to have linear-like structures. Generally, if the average coordination number in a cluster of size  $n$  is  $c$ , the number of bonds is  $nc/2$ . In planar clusters, the average coordination number is larger than 3, which consequently generates a larger number of bonds than the linear-like clusters observed here.

At densities lower than 1.1 g/cm<sup>3</sup>, the coordination numbers (Figure 6) and the numbers of bonds in clusters (Figure 7) do not depend greatly on the density, unlike the numbers of clusters

(Figure 5). This indicates that the coordination number in the connected mass of atoms also approaches 2 as found with clusters.

The number of possible forms for each cluster increases rapidly as the size increases. There are few large clusters (Figure 5) and their analysis inevitably involves a large statistical error, so we focused on small clusters to investigate the distribution of the geometrical forms. The possible forms of clusters with  $n = 3, 4,$  and  $5$  are illustrated in Figure 8. The number under each cluster figure indicates the number of bonds, and a distinguishing letter is attached. Most of the linear and quasi-linear clusters observed in this study were not observed at low temperatures.<sup>14,15</sup> As for the charge of clusters, it is technically difficult to investigate the charge distribution for all the MD steps. However, charge separation was unlikely to occur because the clusters frequently interacted with each other and changed formation.

The distributions of these clusters are shown in Figure 9. The statistics were sampled and averaged over 16000 time steps. The cluster distributions were uniform in the unit cells. When  $n = 3$ , the linear cluster (2) dominates about 70–80% of the distribution and the ratio does not depend greatly on the temperature. This explains why the number of bonds is close to 2 as seen in Figure 7. The linear structure is preferred because it has a low free energy at these high temperatures. When a bond is cut, the cluster gains a large degree of freedom, i.e., a high entropy value. Although some bonding energy may be lost, a high entropy value is beneficial in terms of reducing the free energy under high temperature conditions.

When  $n = 4$ , the linear cluster (3a) occupies about 50–60%, and the planar cluster (5), which is considered to be the most stable at zero temperature, occupies only about 10%. Cluster (4a) is considered to be both linear and planar. The ring-shaped cluster (4b) and the three-dimensional cluster (6) rarely appear at these temperatures. This is probably because these structures have less binding energy and less degree of freedom than a planar cluster (5).

When  $n = 5$ , relatively large statistical errors are involved at 8000 K. However, it is observed that the linear cluster (4a) occupies the largest portion of about 30% at 10000 and 12000 K. Clusters (4b) and (5a) can be regarded as semilinear, and the sum of (4a), (4b), and (5a) occupies about 50–70%. For the same reason as when  $n = 4$ , the ring-shaped cluster (5e) rarely appears. Clusters with seven or more bonds account for less than about 5%. These cluster distributions again explain the small numbers of bonds in Figure 7.

Except when  $n = 5$  at 8000 K, where the statistical error is large, the distribution of the geometrical forms of clusters does not depend greatly on the density because it is determined solely by the difference between the free energy values of each cluster. It should depend on the temperature, but the difference appears to be less than the statistical error in the present cases. As seen in Figures 5–9, boron clusters prefer one-dimensional forms, unlike those at zero temperature. At high temperatures around the liquid–gas CP, the entropy term becomes dominant over the binding-energy term thus reducing the free energy. The result is that a large proportion of the clusters prefers one-dimensional forms to two- or three-dimensional forms.

## Conclusions

The electronic DOS of liquid boron appears to be metallic over a wide atomic density range. This supports earlier

calculations at normal density performed by Vast et al. Since the DOS does not depend greatly on the density, the discrepancy with respect to the conductivity experiment undertaken by Glorieux et al. probably arises from the fact that the states near the Fermi level consist mainly of localized dangling bonds.

The formation of clusters in expanded liquid boron near the CP occurs in quite a different way from that at low temperatures. As the density is reduced, the peak of the coordination number distribution approaches 2, indicating that the clusters prefer one-dimensional geometries to two-dimensional geometries, which are known to be the ground states at low temperatures. This is because one-dimensional geometries are more flexible and have a higher entropy value than two-dimensional geometries. Since the temperature is very high at the CP, the entropy contribution to the free energy becomes larger than the binding energy contribution. The three-dimensional cluster ratio is very small under this condition because three-dimensional clusters are unfavorable as regards to both entropy and binding energy.

## References and Notes

- (1) *Boron, Metallo-Boron Compounds and Boranes*; Adams, R. M., Ed.; Interscience Publishers, John Wiley & Sons: New York, 1964.
- (2) Nagamatsu, J.; Nakagawa, N.; Muranaka, T.; Zenitani, Y.; Akimitsu, J. *Nature (London)* **2001**, *410*, 63.
- (3) Eremets, M. I.; Struzhkin, V. V.; Mao, H.; Hemley, R. J. *Science* **2001**, *293*, 272.
- (4) Ciuparu, D.; Klie, R. F.; Zhu, Y.; Pfefferle, L. *J. Phys. Chem. B* **2004**, *108*, 3967.
- (5) Boustani, I.; Quandt, A.; Hernández, E.; Rubio, A. *J. Chem. Phys.* **1999**, *110*, 3176.
- (6) Krishnan, S.; Nordine, P. C.; Weber, J. K. R.; Schiffman, R. A. *High Temp. Sci.* **1991**, *31*, 45.
- (7) Vast, N.; Bernard, S.; Zerah, G. *Phys. Rev. B* **1995**, *52*, 4123.
- (8) Beckel, C. L.; Yousaf, M.; Fuka, M. Z.; Raja, S. Y.; Lu, N. *Phys. Rev. B* **1991**, *44*, 2535.
- (9) Shirai, K.; Gonda, S. *J. Phys. Chem. Solids* **1996**, *57*, 109.
- (10) Krishnan, S.; Ansell, S.; Felten, J. J.; Volin, K. J.; Price, D. L. *Phys. Rev. Lett.* **1998**, *81*, 586.
- (11) Millot, F.; Rifflet, J. C.; Sarou-Kanian, V.; Wille, G. *Int. J. Thermophys.* **2002**, *23*, 1185.
- (12) Paradis, P. F.; Ishikawa, T.; Yoda, S. *Appl. Phys. Lett.* **2005**, *86*, 151901.
- (13) Glorieux, B.; Saboungi, M. L.; Enderby, J. E. *Europhys. Lett.* **2001**, *56*, 81.
- (14) Boustani, I. *Phys. Rev. B* **1997**, *55*, 16426.
- (15) Zhai, H. J.; Kiran, B.; Li, J.; Wang, L.-S. *Nat. Mater.* **2003**, *2*, 827.
- (16) *CPMD*. Copyright IBM Corp. 1990–2004, Copyright MPI für Festkörperforschung Stuttgart 1997–2001, <http://www.cpmd.org/>.
- (17) Marx, D.; Hutter, J.; *Modern Methods and Algorithms of Quantum Chemistry Proceedings*; NIC Series Vol. 1; John von Neumann Institute for Computing: Jülich, 2000; pp 301–449.
- (18) Hohenberg, P.; Kohn, W. *Phys. Rev.* **1964**, *136*, B864.
- (19) Kohn, W.; Sham, L. J. *Phys. Rev.* **1965**, *140*, A1133.
- (20) Car, R.; Parrinello, M. *Phys. Rev. Lett.* **1985**, *55*, 2471.
- (21) Troullier, N.; Martins, J. L. *Phys. Rev. B* **1991**, *43*, 1993.
- (22) Becke, A. D. *Phys. Rev. A* **1988**, *38*, 3098.
- (23) Lee, C.; Yang, W.; Parr, R. G. *Phys. Rev. B* **1988**, *37*, 785.
- (24) Hayami, W.; Tanaka, T.; Otani, S. *J. Phys. Chem. A* **2005**, *109*, 11975.
- (25) Parrinello, M.; Rahman, A. *Phys. Rev. Lett.* **1980**, *45*, 1196.
- (26) Focher, P.; Chiarotti, G. L.; Bernasconi, M.; Tosatti, E.; Parrinello, M. *Europhys. Lett.* **1994**, *26*, 345.
- (27) Nielsen, O. L.; Martin, R. M. *Phys. Rev. Lett.* **1983**, *50*, 697.
- (28) Hensel, F. *J. Phys.: Condens. Matter* **1990**, *2*, SA33.
- (29) Johanson, J. K.; Zollweg, J. A.; Gubbins, K. E. *Mol. Phys.* **1993**, *78*, 591.
- (30) Lee, S.; Bylander, D. M.; Kleinman, L. *Phys. Rev. B* **1990**, *42*, 1316.